

Inference of Upcoming Human Grasp Using EMG During Reach-to-Grasp Movement

Mo Han, Mehrshad Zandigohar, Sezen Yağmur Günay, Gunar Schirner, and Deniz Erdoğmuş

arXiv:2104.09627v2 [cs.RO] 14 Mar 2022

Abstract—Electromyography (EMG) data has been extensively adopted as an intuitive interface for instructing human–robot collaboration. A major challenge of the real-time detection of human grasp intent is the identification of dynamic EMG from hand movements. Previous studies mainly implemented steady-state EMG classification with a small number of grasp patterns on dynamic situations, which are insufficient to generate differentiated control regarding the muscular activity variation in practice. In order to better detect dynamic movements, more EMG variability could be integrated into the model. However, only limited research were concentrated on such detection of dynamic grasp motions, and most existing assessments on non-static EMG classification either require supervised ground-truth timestamps of the movement status, or only contain limited kinematic variations. In this study, we propose a framework for classifying dynamic EMG signals into gestures, and examine the impact of different movement phases, using an unsupervised method to segment and label the action transitions. We collected and utilized data from large gesture vocabularies with multiple dynamic actions to encode the transitions from one grasp intent to another based on common sequences of the grasp movements. The classifier for identifying the gesture label was constructed afterwards based on the dynamic EMG signal, with no supervised annotation of kinematic movements required. Finally, we evaluated the performances of several training strategies using EMG data from different movement phases, and explored the information revealed from each phase. All experiments were evaluated in a real-time style with the performance transitions over time presented.

Index Terms—electromyography (EMG) signals, dynamic EMG, gesture classification, human intent inference, machine learning

I. INTRODUCTION

COLLABORATIVE robotics have been widely utilized in assistive environment and smart prosthetic hand, with the rapid development of human–robot interaction (HRI) technology. The activity detection of human hand and arm [1] is an intuitive interface for instructing the cognitive collaboration between human and robot, without requiring users to have professional control skills. To extract the motion instructions, electromyography (EMG) signal collected from arm and hand

The authors are with the Department of Electrical and Computer Engineering, Northeastern University, Boston, MA 02115, USA. E-mail: {han.m, zandigohar.m, gunay.s, g.schirner, d.erdogmus}@northeastern.edu.

This work is partially supported by NSF (CPS-1544895, CPS-1544636, CPS-1544815).

has been extensively adopted since it can accurately detect the motion intention and does not require invasive data collection [2–4].

Online human–robot interaction through hand and arm motion is complex to achieve due to the high degrees of freedom (DOFs) of human body structure. More specifically, the human hand alone consists of 21 DOFs controlled by 29 muscles [5]. Most previous studies focused on investigating the discrete classifications of hand and arm movements, by exploiting the mapping between EMG signals and hand postures [2–4], [6–8]. However, this is insufficient to generate differentiated control regarding to the variety of practical dynamic EMG signal. In real-world applications, the muscular activity varies between a static and a dynamic arm position, and the hand configuration also changes simultaneously with the arm motion [9]. Moreover, those studies have only considered a small number of grasp patterns, which cannot ensure the model robustness as required by the grasping of a larger variety of objects. To improve the control effectiveness and user comfort, human intention should be detected in a more dynamic, natural and smooth manner.

In order to increase the system applicability to a wider range of movements, one could integrate more EMG variability into the model training and validation using transient EMG signals from different dynamic phases [10], [11]. Furthermore, the hand motions are commonly carried out in concert with the dynamic movements of arm. For example, when the hand is approaching a target object to be grasped, the configuration of the fingers and wrist also changes simultaneously during the reach-to-grasp motion according to the shape and distance of the object [12]. Therefore, the identification of varying muscular contractions and dynamic arm postures could provide more response time for pre-shaping the robot, leading to improved system usability and more natural grasp transitions.

However, only limited research were focused on detecting dynamic grasp motions [13–15]. Among those works, researchers in [13] proposed an EMG-based learning approach to decode dynamic reach-to-grasp movements by measuring the ground-truth finger configurations with a wired glove. Authors of [14] also explored a classifier to identify transient anticipatory EMG signal incorporating dynamic grasp actions, with the ground-truth timestamps of action transitions detected by a kinematic device. In [15], the grasp classification was evaluated on data involving both static and dynamic contractions, but the data collection experiments were actually conducted in a discrete manner, where the subjects were required



Fig. 1: Visualization of muscles targeted during experiment.

to maintain the grasping and resting positions alternately for specified time lengths, so the practical movement continuity was still missing. In other word, most existing assessments on non-static EMG classification either require the supervised ground-truth timestamps of the movement status, or only contain limited dynamic variations of the EMG signal.

Therefore, we propose a framework for classifying dynamic EMG signals into gestures, and examine the impact of different phases of reach-to-grasp movements on final performance. We exploit the continuity of hand formation change to increase data variability, and decode the subject grasping intention in a real-time manner. We utilized EMG data from large vocabularies of gestures with multiple dynamic motion phases, in order to encode the transitions from one intent to another based on common sequences of reach-to-grasp movements. During the data collection, continuous variations on multi-scale muscular contractions were introduced by the designed experiment protocol simulating the actual situation. We segmented the continuous EMG data unsupervisedly into different dynamic motion sequences, and further labeled those EMG sequences according to the specific motion. Classifier for identifying gesture label was constructed afterwards based on the dynamic EMG signal, with no supervised annotation of kinematic movements required. Finally, we examined the performances of several training strategies using EMG data from different dynamic phases, and explored the information revealed from each phase. All experiments were evaluated in a real-time style with the performance variation over time presented, and the proposed method was shown to be efficient due to the higher data variations.

II. EXPERIMENTAL PROTOCOL AND DATA PROCESSING

The utilized data were collected from 5 healthy subjects (4 male, 1 female; mean age: 26.7 ± 3.5 years). All subjects were right-handed and only dominant hand was used for the data collection. None of the subjects had any known motor or psychological disorders. The experimental procedure and task were explained to all subjects and their consents to the participation were taken.

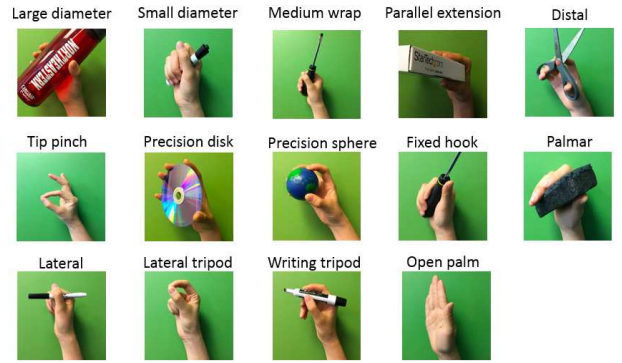


Fig. 2: Selected 14 gestures for the classification problem.

A. EMG Sensor Configurations

We collected surface EMG (Motion Lab Systems, Baton Rouge, LA, USA) in bipolar derivations, with a sampling rate of $f = 1562.5$ Hz. The visualization of the $C = 12$ targeted muscles of our experiment is shown in Fig. 1, including muscles ranging from hand to upper arm in order to capture more dynamic movement information. The 12 muscles are: First Dorsal Interosseous (FDI), Abductor Pollicis Brevis (APB), Flexor Digiti Minimi (FDM), Extensor Indicis (EI), Extensor Digitorum Communis (EDC), Flexor Digitorum Superficialis (FDS), Brachioradialis (BRD), Extensor Carpi Radialis (ECR), Extensor Carpi Ulnaris (ECU), Flexor Carpi Ulnaris (FCU), Biceps Brachii Long Head (BIC), and Triceps Brachii Lateral/Short Head (TRI).

B. Experimental Protocol

The experimental protocol focused on 14 gestures and 4 dynamic motion phases involving commonly used gestures and wrist motions [16]. As shown in Fig.2, the 14 classes were: large diameter, small diameter, medium wrap, parallel extension, distal, tip pinch, precision disk, precision sphere, fixed hook, palmar, lateral, lateral tripod, writing tripod, and open palm/rest. We defined the 14 grasp labels as $l \in \{0, 1, \dots, 13\}$, where $l = 0$ indicated the open-palm/rest gesture without any movement, and $l \in \{1, \dots, 13\}$ were accordingly identified as the other 13 gestures listed in Fig.2.

Each subject participated in two collection sessions in total, involving the task to lift and move different objects from one position to the another, where in the first session the object was moved in a clockwise trajectory while the second session was in counterclockwise. The subject was allowed to rest for fifteen minutes between the two sessions.

During the session, each gesture of $l \in \{1, \dots, 13\}$ (not including the open-palm/rest gesture) was performed four times with four different objects, leading to 52 objects totally in each session. The subject performed 6 trials for each of the 52 objects per session, where each trial was executed along its corresponding predefined path, as shown in Fig.3. During the first trial t_1 , the object was moved from the initial position P_0 to the position P_1 , followed with another five trials to move the object clockwise until it was returned to the initial position P_0 . The counterclockwise session was performed in a similar manner as Fig.3 but in a different direction with respect to

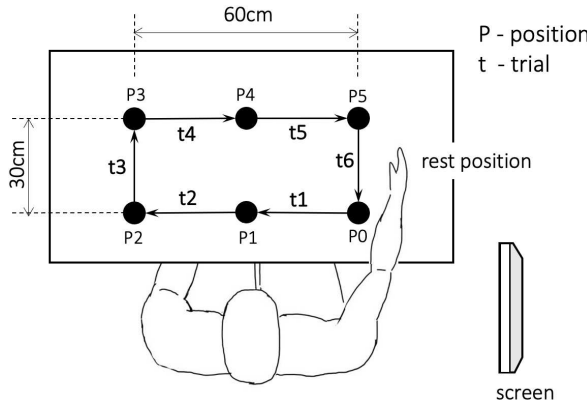


Fig. 3: Vertical view of experimental setup for the session of moving object clockwise, where P is defined as the object position and t is defined as each trial. Subject performed 6 trials per object, where each trial was executed along its corresponding predefined path represented by arrows from one position to another. The object was first moved from the initial position P_0 to the position P_1 during trial t_1 , followed with another five trials to move the object clockwise until it was returned to the initial position P_0 .

the initial position P_0 . Therefore, the grasp movement could be conducted from different angles, directions and distances towards the target subject, introducing more variety into the collected dynamic EMG data.

At the beginning of the experiment, subject was seated facing a table and electrodes were connected to the right arm while the arm was at the rest position with an open palm, as illustrated in Fig.3. Object center configuration was defined with 6 marks on the table. A screen was placed at the right side of subject for showing example picture of the gesture to be executed. First, the subject was given 5 seconds to read the gesture shown on the screen, followed with an audio cue illustrating the beginning of the first trial. Each trial lasted for 4 seconds, and the object was grasped and moved along its predefined path using the designated gesture for 6 trials without interruption, with audio cues given between different trials. Within each 4-second trial, the subject was required to complete 4 actions which could be naturally performed by human during reach-to-grasp movements, including: (1). reaching (reaching the object), (2). grasping (grasping to move the object), (3). returning (returning to the rest position), and (4). resting (resting at the rest position with open palm). The complete timeline for grasping each object is presented in Fig.4. Note that for each trial, the four grasp phases (reaching, grasping, returning and resting) were performed freely and naturally by the subject without limitation on the speed of each phase as long as all the 4 phases were completed within 4 seconds, in order to preserve sufficient information of the dynamic motion.

C. Data Pre-Processing

Since the experimental procedure requires subjects to execute real movements, the data is prone to noises and motion artifacts. Thus, we applied fourth-order band-pass (40

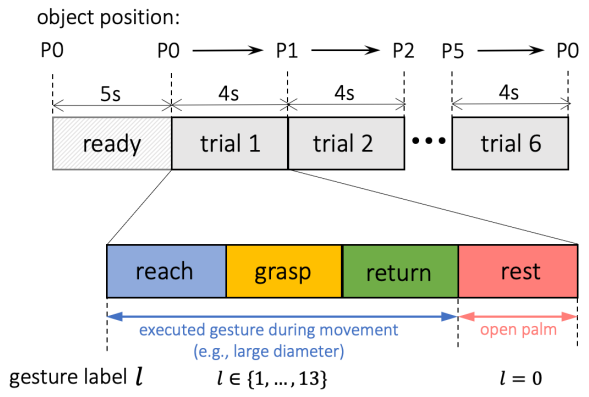


Fig. 4: Experiment timeline and the EMG segmentation and annotation. First the subject was given 5 seconds to read the shown gesture, followed with an audio cue for starting the first trial. Each trial lasted for 4 seconds, and the grasp was performed for 6 continuous trials without interruption, between which audio cues were given. Each EMG trial was further segmented unsupervisedly into four sequences corresponding to four dynamic motion phases. Then the first three motion phases were labeled as gesture $l \in \{1, \dots, 13\}$ corresponding to the current target object, and the resting phase was tagged by the open-palm label $l = 0$.

Hz to 500 Hz) Butterworth filter to remove the unwanted contamination and clear any other frequency noise outside of the normal EMG range. No default filtering was applied to the data from the acquisition device.

Due to the nature of human muscle system, upper arm muscles generate stronger signals than hand muscles and thus a fair source contribution would be only possible by normalizing each muscle with respect to its maximum power. Therefore, the maximum voluntary contraction (MVC) test was conducted and recorded for each muscle where the subjects were asked to perform isometric contractions of muscles lasting for 3 seconds. The envelope of both the experiment and the MVC data were generated, and each channel of the experiment data were then normalized with respect to the maximum value of MVC envelopes.

In order to implement the EMG identification in real-time, we further divided the processed experiment data of EMG envelopes into sliding time windows of $T = 320$ ms, with a step size of 40 ms between two consecutive windows. The following EMG feature extraction and classification were all conducted based on each time window.

III. METHODOLOGIES

A. Feature Extraction

The selection of EMG feature requires to consider both processing time and data representability while avoiding redundancy to maximize the classification performance [17]. The time-domain features require lower computational complexity compared to frequency-domain features and thus can be implemented in real-time with higher speed [17]. In this study, three time domain features were extracted, including root mean square (RMS), mean absolute value (MAV), and

variance of EMG (VAR). As illustrated in [18], maximum likelihood estimation of EMG amplitude can be evaluated by RMS feature, since under constant-force, constant-angle, and non-fatiguing contraction EMG signals can be modelled with Gaussian distributions. Additionally, MAV is a common feature for indicating EMG amplitude due to low computational requirements and potential for higher class distinction [19], [20]. Lastly, previous experimental studies also showed that VAR feature could improve the EMG classification performance, which is another frequently used feature in EMG classification studies [17], [19].

The pre-processed EMG time windows were transferred to the feature extraction step, and RMS, MAV and VAR features were calculated over the window input of $X \in \mathbb{R}^{C \times T}$, where $C = 12$ is the channel number of EMG from all muscles and $T = 320$ ms is the window length with a sampling rate of $f = 1562.5$ Hz. Then the output feature vector of $Z \in \mathbb{R}^{3C \times 1}$ was yielded corresponding to each input window $X \in \mathbb{R}^{C \times T}$.

B. Unsupervised Segmentation of Dynamic Motion

In each trial, the grasp movements were performed naturally by subject without limitation on the timing of each motion phase. Since the distances between hand and object varied across different trials, the lengths of EMG sequences from different motion phases were also not constant. For example, as shown in Fig. 3, the reaching movement of trial t1 was longer than that of t3, since the object was closer to the hand during t1. Therefore, to approach the gesture classification in a continuous manner, we first segmented each EMG trial into different movement sequences unsupervisedly, and then labeled those sequences separately according to the specific motion, as shown in Fig.4.

To segment each EMG trial into multiple sequences unsupervisedly based on the dynamic grasp movements, the method of Greedy Gaussian Segmentation (GSS) [21] was adopted. The GSS algorithm works under the assumption that during a particular static state, the EMG signal can be well explained as a Gaussian random process with zero mean [22]. This GSS method aims to break down multivariate time series into several segments, where the observed data in different segments can be well modeled as separate Gaussian distributions which are independent from the other segments. Therefore, the mean and covariance of the Gaussian distribution in each segment are also assumed to be unrelated to the other segments. This time-series segmentation task can then be transformed into a maximum likelihood problem, where the optimal solution is a set of breakpoints maximizing the overall likelihood when sampling from all of the independent Gaussian segments. To decrease the computation time, GSS utilizes a greedy and scalable implementation of dynamic programming where optimal breakpoints are calculated iteratively and re-adjusted in each iteration.

In this work, we segmented each EMG trial using GSS, by assigning 3 breakpoints to each trial leading to 4 sequences corresponding to reaching, grasping, returning and resting. By doing so, the order of different movement phases was taken into account by imposing higher probability to movement transitions that were expected to follow one another, e.g. grasping

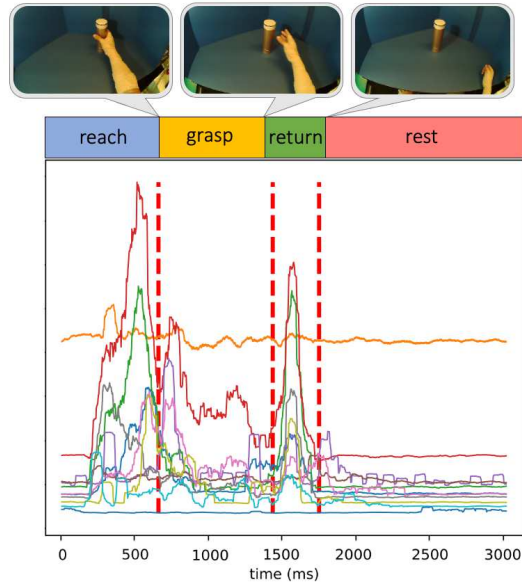


Fig. 5: An example of unsupervised segmentation of dynamic EMG signal using the GGS algorithm, where the EMG signal includes $C = 12$ channels and the red dashed lines represent the locally optimal segment boundaries. Each of the four segmented EMG sequences was modeled as an independent multivariate Gaussian distribution with different means and variances. Three key frames of the experiment video corresponding to the three segment boundaries are also shown.

movement following reaching movement, later followed by returning action. Given the specified number of breakpoints, GSS algorithm was utilized to unsupervisedly segment the EMG trial and provide the optimal segment boundaries.

In Fig.5, such utilization of GSS method is depicted, where each segment of the 12-channel EMG series is modeled as an independent multivariate Gaussian distribution with distinct mean and covariance parameters. During the data collection, an eye-tracker was also worn by the subject, where experiment videos synchronized to the EMG data were recorded by the forward-facing world camera of the eye-tracker. In order to validate the effectiveness of the unsupervised segmentation, for each trial we extracted and reviewed three key video frames corresponding to the three segment boundaries, to make sure the hand movements shown in the frames are consistent with the motion phase transitions. An example of such experiment key frames is displayed in Fig.5, where the hand just reached the object without lifting it at the first break point, the hand just released the object and started returning at the second break point, and finally the hand returned to the rest position at the last break point.

C. Dynamic Hand Gesture Annotation

Throughout the reach-to-grasp movement, the limb configurations of fingers and wrist change in concert continuously with respect to the shape and distance of the targeted object [12]. A closer look would reveal the fact that humans tend to pre-shape their hand prior to touching the targeted object. In order to recognize these hand gestures based on

the upcoming dynamic data, we annotated the collected EMG with a set of gesture labels $l \in \{0, 1, \dots, 13\}$, where $l = 0$ was defined as open-palm/rest gesture and $l \in \{1, \dots, 13\}$ were accordingly identified as the other 13 gestures listed in Fig.2. Based on this definition, following the segmented EMG trials as shown in Fig.4, we labelled the three motional EMG sequences of reaching, grasping and returning to be the gesture $l \in \{1, \dots, 13\}$ executed during the movement, and tagged the stationary phase of resting with the open-palm label $l = 0$.

D. Classification of the Dynamic Hand Gesture

We constructed a classifier to recognize dynamic hand gestures using the collected EMG signals. The EMG signals were first broken down into time windows of $X_i \in \mathbb{R}^{C \times T}$ with size $T = 320$ ms ($f = 1562.5$ Hz sampling rate), where X_i represents the i th EMG window and $C = 12$ is number of channels. Then, based on the gesture label $l \in \{0, 1, \dots, 13\}$ of the corresponding EMG window X_i , pairs of data and label $\{(X_i, l)\}_{i=1}^n$ were formed, where n is the total number of windows. Later, the selected three time-domain features of RMS, MAV and VAR were extracted as $Z_i \in \mathbb{R}^{3C \times 1}$ for each EMG window $X_i \in \mathbb{R}^{C \times T}$, leading to feature and label pairs of $\{(Z_i, l)\}_{i=1}^n$.

In this work, we utilized the extra-trees method [23] for identifying hand gestures based on the extracted EMG features. This method incorporates the averaging of an ensemble of random decision trees trained on different sub-samples of the dataset, in order to reduce overfitting and improve performance. We observed that the utilization of extra-trees algorithm with a combination of 50 trees provided desirable performance, hence used in this work.

E. Training and Validation

We performed inter-subject training and validation of the 14-class gesture classification. For every subject, we randomly split the 6 trials collected from each object into 4 training trials and 2 validation trials, leading to 224 trials (66.7%) for training and 112 trials (33.3%) for validation in total. Thereafter, the classifier was trained on the aforementioned training set and evaluated on the left-out validation set which was unseen to the classifier. Since our main objective was to detect the upcoming grasping intention at an earlier stage and pre-shape the robot before the final grasp accomplished, the data from returning phase was excluded from training, during which the grasp was already completed and the object was already released from hand. However, to provide a full scope of the effectiveness of the classification approach, the classifier was then evaluated on the entire EMG trial of four movement phases irrespectively.

As the subjects were not required to perform the four movement phases of reach-grasp-return-rest in a fixed timing or speed during the data collection, the length of each phase for different trials varies based on the subject's natural pace. Therefore, during the evaluation, we aligned all validation EMG trials based on the breakpoint occurring at the beginning of the grasping phase, as shown at 0ms in Fig.6. In this way, the evaluation could focus more on the assessment of transition

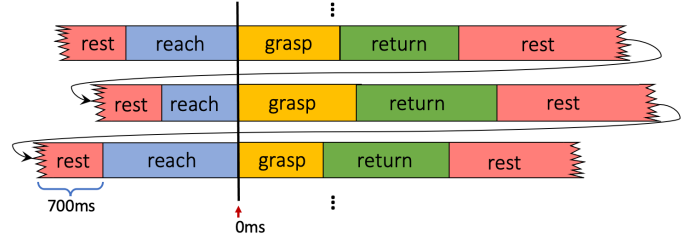


Fig. 6: Time alignment for EMG windows of validation trials.

from reaching to grasping, which is the key transition in grasp intent inference. Therefore, the overall validation performance can be integrated more clearly by averaging across all aligned validation trials. As the last step, the resting-phase data of 700ms from the end of previous trial was appended at the beginning of its following trial in order to show the dynamic transition between resting and reaching phases.

IV. EXPERIMENTAL EVALUATION AND RESULTS

As mentioned earlier, we trained the classifier with reaching, grasping and resting phases only, whereas validated the model with all motion phases (reaching, grasping, returning and resting). In order to specifically inspect the performance of the dynamic-EMG classifier and explore the informative levels of EMG data from different motion phases, the constructed gesture classifier was trained with three different strategies independently:

- 1) Trained with EMG of reaching and resting phases;
- 2) Trained with EMG of grasping and resting phases;
- 3) Trained with EMG of reaching, grasping and resting phases.

The classifier performances trained with those three strategies are shown in Fig. 7, Fig. 8 and Fig. 9, respectively. We present the validation results as functions of time, in order to inspect the performance variation during different dynamic phases within a trial. In those figures, the predicted probabilities and accuracy on validation set are respectively shown, where each time point represents a EMG window and the performances are averaged within the same window over all validation trials given the aligned timeline. The beginning of the grasping phase is marked as 0ms, and the averaged breakpoints between different motion phases are illustrated by vertical dashed lines. The *grasp gesture* is defined as the executed gesture $l \in \{1, \dots, 13\}$ during the non-resting phases, the *rest gesture* represents the open-palm/rest gesture $l = 0$ during the resting phase, and the *top competitor* is identified as the gesture with the highest probability among the other 12 gestures except for the *grasp gesture* and *rest gesture*. In Fig. 7, 8, 9 (a), the time point at which the probability curves of *grasp gesture* and *rest gesture* intersect with each other is defined as t_i (the intersection is marked by a solid red dot), and the distance from the probability peak of *grasp gesture* to the simultaneous probability of *top competitor* is defined as d_p . In Fig. 7, 8, 9 (b), the accuracies of successfully detecting the *grasp gesture* and *rest gesture* are independently given.

In this section, performances of the three training strategies were further compared and analyzed, and the information

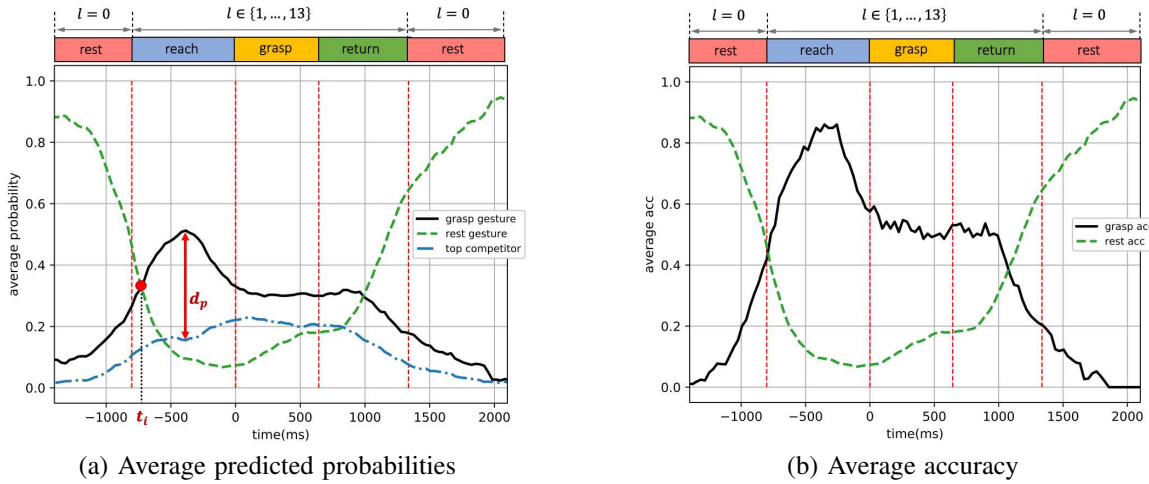


Fig. 7: Dynamic-EMG gesture classifier trained by the first strategy (reaching and resting phases): predicted probabilities and accuracy on validation set, presented as functions of time.

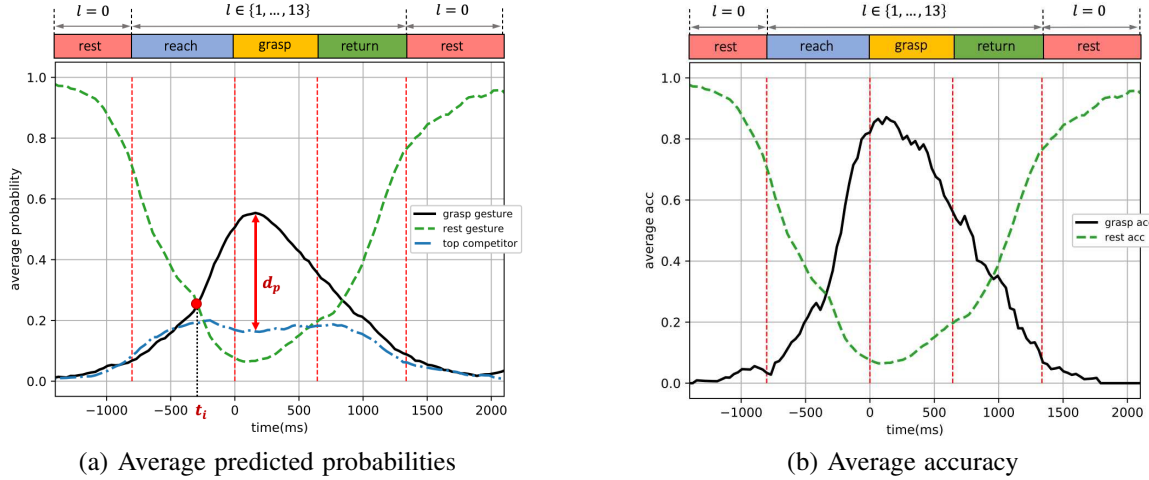


Fig. 8: Dynamic-EMG gesture classifier trained by the second strategy (grasping and resting phases): predicted probabilities and accuracy on validation set, presented as functions of time.

revealed by dynamic EMG of different motion phases were also discussed.

A. Training with Reaching and Resting Phases

The performance of the classifier trained by the first strategy (reaching and resting phases) is shown in Fig. 7. As illustrated in Fig. 7 (a), since the classifier was trained by reaching phase only without grasping phase, the peak of the *grasp gesture* probability was achieved within reaching phase at around 0.51. During the grasping phase and first half of the returning phase, the *grasp gesture* probability was stable at around 0.3, and then gradually decreased as the movement converted to resting phase. Notably, the probability of *grasp gesture* was constantly higher than *top competitor* through the entire trial. The time point when the probability curves of *grasp gesture* and *rest gesture* intersected was $t_i = -729$ ms, and the distance from the probability peak of *grasp gesture* to the *top competitor* probability was $d_p = 0.36$. Simultaneously, the predicted probability of the *rest gesture* first reduced dramatically to the

value lower than 0.2 as the grasp movement happened, until the hand returned to the resting position when the open-palm probability gradually went up again.

In Fig. 7 (b), the averaged accuracy for detecting *grasp gesture* during reaching phase presented an outstanding performance with a peak over 0.8, and remained higher than 0.6 within most of the reaching phase. This accuracy dropped in grasping and returning phases, fluctuating around 0.5. The performance of detecting *rest gesture* was highly accurate, with the accuracy value over 0.8 throughout most of the two resting phases.

We are especially interested in the intersection point t_i between the *grasp gesture* and *rest gesture* probabilities. Since after this point, the *grasp gesture* starts to outperform the *rest gesture*, and the system could start to prepare for pre-shaping the robot from this point on according to the detected *grasp gesture*. Ideally, this intersection is expected to appear right at the junction where the resting phase ends and the reaching phase starts in order to indicate the beginning of the hand

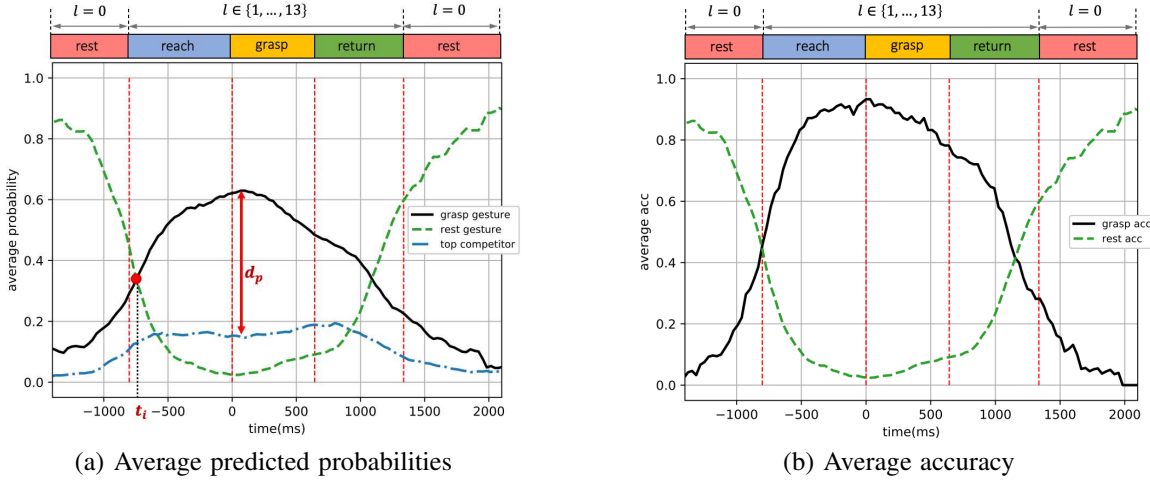


Fig. 9: Dynamic-EMG gesture classifier trained by the third strategy (reaching, grasping and resting phases): predicted probabilities and accuracy on validation set, presented as functions of time.

motion. However, in practice, the hand movement could only be predicted based on the past motion, so the intersection is expected to be after the start of the reaching phase but as close to it as possible. In Fig. 7 (a), the intersection of the two curves appeared $t_i = -729$ ms earlier than the start of the grasping phase, which was after but very close to the beginning of the reaching phase and allowed enough time to pre-shape the robotic hand before the actual grasp. Therefore, the dynamic EMG of the reaching phase is proved to be informative of forecasting the gesture in advance during the reach-to-grasp movement. Furthermore, even though the model was trained by reaching and resting phases only, the probability of *grasp gesture* was still steadily higher than *top competitor* during all the four dynamic phases, representing the significant hand-shaping information revealed by the movement during reaching phase.

B. Training with Grasping and Resting Phases

The performance of the classifier trained by the second strategy (grasping and resting phases) is shown in Fig. 8. As shown in Fig. 8 (a), the *grasp gesture* probability first gradually increased, until the grasping phase where the probability peak of *grasp gesture* was reached at around 0.56. With the hand movement entered returning and resting phases, the *grasp gesture* probability declined to lower than 0.2. The probability curve of *rest gesture* showed an opposite trend with *grasp gesture* probability - the *rest gesture* probability started from a peak at the first resting phase, then decreased under 0.2 as the grasp movement happened, and then finally reached another peak when the hand went back to rest again. The intersection point between *grasp gesture* and *rest gesture* probabilities appeared at $t_i = -334$ ms, and the probability peak of *grasp gesture* was $d_p = 0.41$ higher than *top competitor* probability at the same time point.

In Fig. 8 (b), the accuracy of detecting *grasp gesture* during the grasping phase performed outstandingly better than other phases, showing a similar pattern with its probability curve in Fig. 8 (a). This *grasp gesture* accuracy was also higher than

0.6 during the end of reaching phase and the entire grasping phase. The *rest gesture* accuracy was similar with the model trained by the first strategy as indicated in Fig. 7 (b).

Compared to the classifier trained by reaching phase (the first strategy, shown in Fig. 7) with $t_i = -729$ ms, the probability intersection of this second-strategy model appeared 395ms later in time, at $t_i = -334$ ms. This illustrates that the EMG data of grasping phase contained less information for detecting gesture in earlier stage compared to the reaching-phase data, and thus the model trained by the second strategy provided less response time for the system. However, the *grasp gesture* probability peak of this second model outperformed the *top competitor* by $d_p = 0.41$, which was 0.05 higher than $d_p = 0.36$ of the first model. This demonstrates that the dynamic EMG from grasping phase is more accurate and confident for decision making during the grasp movement, outperforming other interference options to a larger degree.

C. Training with Reaching, Grasping and Resting Phases

1) Time-Performance Analysis: The performance of the classifier trained by the third strategy (reaching, grasping and resting phases) is shown in Fig. 9. In Fig. 9 (a), the predicted probability of *grasp gesture* increased steadily during the reach-to-grasp movement when the grasp was carried out from the resting status, staying around its peak during the reaching and grasping phases, and then gradually decreased when subject finished the grasp and returned to resting status again. Simultaneously, the predicted probability of *rest gesture* first reduced dramatically below 0.2 during the grasp movement, until the hand returned to the resting position when the *rest gesture* probability progressively increased again. The predicted probability of the *top competitor* was remained stably lower than 0.2, which was constantly outperformed by the *grasp gesture* to a significant degree throughout the entire trial. The intersection of *grasp gesture* and *rest gesture* probabilities happened at $t_i = -743$ ms, and the probability peak of *grasp gesture* was $d_p = 0.49$ higher than the simultaneous *top competitor*.

TABLE I: The summary of model performances trained by the first, second and third training strategy.

Training Phases	t_i	d_p	Prob. Peak
Reach + Rest	-729ms	0.36	Reach
Grasp + Rest	-334ms	0.41	Grasp
Reach + Grasp + Rest	-743ms	0.49	Reach + Grasp

For the dynamic gesture classification, as shown in Fig. 9 (b), the accuracy of *grasp gesture* was stably higher than 0.8 within most of the reaching and grasping phases, which are the most critical phases for making robotic-grasp decision. It is worth noting that, the validation accuracy was still higher than 0.75 at the beginning of the returning phase even though the model was not trained on any data from that phase. The accuracy curve of *rest gesture* presented a similar trend as shown in Fig. 7 (b) and Fig. 8 (b).

Compared to the first and second training strategy, the third training strategy combined the advantages from both reaching and grasping phases, leading to a boosted performance on detecting dynamic EMG compared to each single phase of reaching and grasping. The intersection point $t_i = -743\text{ms}$ moved towards the beginning of reaching phase even closer compared to the first training strategy, and the model was able to distinguish between *grasp gesture* and *top competitor* with higher degree of confidence throughout the entire trial compared to the second training strategy. Therefore, the model could provide even more response time before the grasp happens with more precise performance. Even during the returning phase which was unseen to the training, the model could still perform decently, illustrating the gain of using dynamic EMG for training. This higher degree of freedom in EMG data could enable more information and stability of the model to a wider range postures during the dynamic grasp activity. In addition, the accuracy for detecting resting phase was also highly accurate and sensitive to perform as a detector of muscle activation for triggering the robotic grasp.

The summary of model performances is shown in Table I. In short, the dynamic data from reaching phase could provide more response time for robot pre-shaping before the grasp happens, the dynamic data from grasping phase could improve the decision confidence and robustness regarding to other competitors, and the higher data variability from combining reaching and grasping phases could leverage the advantages from both motion phases and further boost the performance of dynamic-EMG classification.

2) Gesture Classification Confusion Matrix: In order to investigate the model performance regarding to different gestures, in Fig. 10 we plot the confusion matrix of the model trained by the third strategy, which was evaluated on the left-out validation set. Here we only present the evaluation result during the pre-shaping time period from $t = -743\text{ms}$ to $t = 0\text{ms}$, in order to inspect the model capability of detecting upcoming gestures during reaching phase before the actual grasp happens.

As shown in Fig. 10, the model was able to detect the

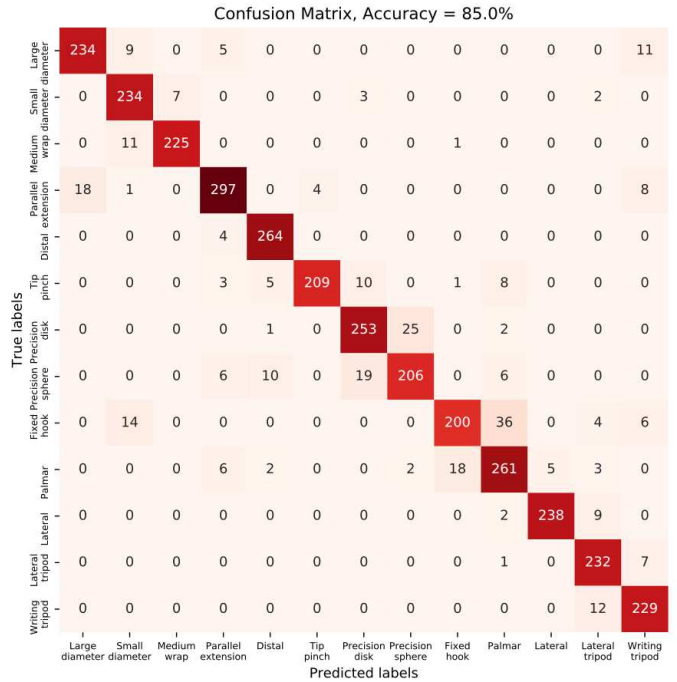


Fig. 10: Confusion matrix of the model trained with the third strategy, during the pre-shaping time period from $t = -743\text{ms}$ to $t = 0\text{ms}$.

upcoming gestures efficiently during the pre-shaping period, with an average accuracy of 85%. In addition, the model could also clearly distinguish between different gestures, even though it was trained with large gesture vocabularies with multiple dynamic motion positions. But there are gesture pairs existing which are less distinguishable as illustrated in Fig. 10, of which one gesture is very similar to the other. For example, precision disk and precision sphere is such a pair, where one of them was predicted wrongly to be the other with higher frequency during the validation. That is because the two gestures have very similar hand configurations but only different opening width during the reach-to-grasp movement, and the precision sphere could even be an intermediate state of the precision disk when the hand slowly opens. Another example of such confusing gesture pair is fixed hook and palmar as presented in Fig. 10, since the thumb postures of the two gestures are very similar, and the difference is only in the finger joint angles which could not be fully detected by the hand/arm muscle. In order to better distinguish the subtle differences between similar gestures, the time period of pre-shaping could even be divided to more detailed sub-phases for capturing preciser changes of the finger configurations.

V. CONCLUSION

In this paper, we proposed a non-static EMG recognition method for identifying real-time hand/arm movements regarding the dynamic muscular activity variation in practice. The presented framework was trained and validated by EMG signals collected from continuous grasp tasks with variations on dynamic hand postures, so that the transitions from one intent to another could be encoded into the model based on common

sequences of the grasp movements. The obtained EMG data was segmented unsupervisedly into different dynamic motion sequences, and further labeled based on the specific motion. A classifier was then constructed for recognizing the gesture label based on the dynamic EMG signal, and the impact of different movement phases were examined via comparative experiments. The proposed method was assessed in a real-time manner and the corresponding performance variation over time was presented. Results illustrated the effectiveness of the framework built with the EMG data of high degree of freedom.

REFERENCES

- [1] S. Sheikholeslami, A. Moon, and E. A. Croft, "Cooperative gestures for industry: Exploring the efficacy of robot hand configurations in expression of instructional gestures for human–robot interaction," *The International Journal of Robotics Research*, vol. 36, no. 5-7, pp. 699–720, 2017.
- [2] M. Han, S. Y. Günay, G. Schirner, T. Padır, and D. Erdoğmuş, "Hands: a multimodal dataset for modeling toward human grasp intent inference in prosthetic hands," *Intelligent service robotics*, vol. 13, no. 1, pp. 179–185, 2020.
- [3] Z. Ju and H. Liu, "Human hand motion analysis with multisensory information," *IEEE/AsMe Transactions on Mechatronics*, vol. 19, no. 2, pp. 456–466, 2013.
- [4] M. Han, S. Y. Günay, İ. Yıldız, P. Bonato, C. D. Onal, T. Padır, G. Schirner, and D. Erdoğmuş, "From hand-perspective visual information to grasp type probabilities: deep learning via ranking labels," in *Proceedings of the 12th ACM international conference on pervasive technologies related to assistive environments*, 2019, pp. 256–263.
- [5] L. A. Jones and S. J. Lederman, *Human hand function*. Oxford university press, 2006.
- [6] F. Sebelius, M. Axelsson, N. Danielsen, J. Schouenborg, and T. Laurell, "Real-time control of a virtual hand," *Technology and Disability*, vol. 17, no. 3, pp. 131–141, 2005.
- [7] S. A. Dalley, H. A. Varol, and M. Goldfarb, "A method for the control of multigrasp myoelectric prosthetic hands," *IEEE Transactions on Neural Systems and Rehabilitation Engineering*, vol. 20, no. 1, pp. 58–67, 2011.
- [8] G. Ouyang, X. Zhu, Z. Ju, and H. Liu, "Dynamical characteristics of surface emg signals of hand grasps via recurrence plot," *IEEE journal of biomedical and health informatics*, vol. 18, no. 1, pp. 257–265, 2013.
- [9] N. Jiang, S. Muceli, B. Graumann, and D. Farina, "Effect of arm position on the prediction of kinematics from emg in amputees," *Medical & biological engineering & computing*, vol. 51, no. 1, pp. 143–151, 2013.
- [10] C. Castellini, P. Artermiadis, M. Winingar, A. Ajoudani, M. Alimusaj, A. Bicchi, B. Caputo, W. Craelius, S. Dosen, K. Englehart *et al.*, "Proceedings of the first workshop on peripheral machine interfaces: Going beyond traditional surface electromyography," *Frontiers in neurorobotics*, vol. 8, p. 22, 2014.
- [11] D. Yang, J. Zhao, L. Jiang, and H. Liu, "Dynamic hand motion recognition based on transient and steady-state emg signals," *International Journal of Humanoid Robotics*, vol. 9, no. 01, p. 1250007, 2012.
- [12] M. Jeannerod, "The timing of natural prehension movements," *Journal of motor behavior*, vol. 16, no. 3, pp. 235–254, 1984.
- [13] I. Batzianoulis, S. El-Khoury, E. Pirondini, M. Coscia, S. Micera, and A. Billard, "Emg-based decoding of grasp gestures in reaching-to-grasping motions," *Robotics and Autonomous Systems*, vol. 91, pp. 59–70, 2017.
- [14] H. C. Siu, J. A. Shah, and L. A. Stirling, "Classification of anticipatory signals for grasp and release from surface electromyography," *Sensors*, vol. 16, no. 11, p. 1782, 2016.
- [15] T. Lorrain, N. Jiang, and D. Farina, "Influence of the training set on the accuracy of surface emg classification in dynamic contractions for the control of multifunction prostheses," *Journal of neuroengineering and rehabilitation*, vol. 8, no. 1, pp. 1–9, 2011.
- [16] T. Feix, J. Romero, H.-B. Schmidtmayer, A. M. Dollar, and D. Kragic, "The grasp taxonomy of human grasp types," *IEEE Transactions on Human-Machine Systems*, vol. 46, no. 1, pp. 66–77, 2016.
- [17] A. Phinyomark, P. Phukpattaranont, and C. Limsakul, "Feature reduction and selection for emg signal classification," *Expert systems with applications*, vol. 39, no. 8, pp. 7420–7431, 2012.
- [18] N. Hogan and R. W. Mann, "Myoelectric signal processing: Optimal estimation applied to electromyography-part i: Derivation of the optimal myoprocessor," *IEEE Transactions on Biomedical Engineering*, no. 7, pp. 382–395, 1980.
- [19] A. Phinyomark, S. Hirunviriya, C. Limsakul, and P. Phukpattaranont, "Evaluation of emg feature extraction for hand movement recognition based on euclidean distance and standard deviation," in *ECTI-CON2010: The 2010 ECTI International Conference on Electrical Engineering/Electronics, Computer, Telecommunications and Information Technology*. IEEE, 2010, pp. 856–860.
- [20] A. Phinyomark, C. Limsakul, and P. Phukpattaranont, "Application of wavelet analysis in emg feature extraction for pattern classification," *Measurement Science Review*, vol. 11, no. 2, p. 45, 2011.
- [21] D. Hallac, P. Nystrup, and S. Boyd, "Greedy gaussian segmentation of multivariate time series," *Advances in Data Analysis and Classification*, vol. 13, no. 3, pp. 727–751, 2019.
- [22] E. A. Clancy and N. Hogan, "Probability density of the surface electromyogram and its relation to amplitude detectors," *IEEE Transactions on Biomedical Engineering*, vol. 46, no. 6, pp. 730–739, 1999.
- [23] P. Geurts, D. Ernst, and L. Wehenkel, "Extremely randomized trees," *Machine learning*, vol. 63, no. 1, pp. 3–42, 2006.